***Survival, Movement, and Lifespan: Decoding the Roles of Patched-Related (Ptr) in Drosophila melanogaster***

Cristina Parada [1,2,3], Rafael Cantera [2] and Daniel Prieto [2,4,*]

**1** Departamento de Neurofarmacología Experimental, Instituto de Investigaciones Biológicas Clemente Estable, Montevideo, Uruguay.

**2** Departamento de Biología del Neurodesarrollo, Instituto de Investigaciones Biológicas Clemente Estable, Montevideo, Uruguay.

**3** Programa de Desarrollo de las Ciencias Básicas (PEDECIBA), Uruguay

**4** Departamento de Neurofisiología Celular y Molecular, Instituto de Investigaciones Biológicas Clemente Estable, Montevideo, Uruguay.

* To whom correspondence should be addressed (dprieto@fcien.edu.uy)

## Abstract

Patched-related (Ptr) is a transmembrane protein implicated in developmental processes in *Drosophila melanogaster*, yet its precise role remains incompletely understood. Here, we use $Ptr^{23c}$ null mutants to investigate the functional significance of Ptr through the entire life cycle monitoring survival during embryonic, larval, pupal and adult development, and studying larval locomotion and muscle structure. We report that $Ptr^{23c}$ larvae displayed impaired hatching, indicative of defective embryonic development. Moreover, mutant larvae exhibited reduced mobility and lethargy, suggesting a potential involvement of Ptr in neuromuscular function. Morphological analysis of somatic muscles in mutant larvae revealed enlarged cell nuclei. Despite high pre-adult mortality, a subset of $Ptr^{23c}$ mutant adults display an unexpected extension in lifespan compared to controls, implicating Ptr in the regulation of longevity. Our findings provide critical insights into the multifaceted role of Ptr in *Drosophila* development, highlighting its contributions to post-embryonic survival, neuromuscular function, and lifespan regulation. This study underscores the significance of exploring broader genetic networks to unravel the complexities of developmental processes.

**Keywords:** Patched-related (Ptr), development, survival, muscle, larval locomotion, lifespan.

## Introduction

Patched-related (Ptr) is a multipass transmembrane protein related to the canonical receptor of the Hedgehog (Hh) pathway, Patched (Ptc) (Pastenes et al., 2008). Ptr is ubiquitously present at every stage of *Drosophila melanogaster* development (Bolatto et al., 2022, 2015; Pastenes et al., 2008). The expression of *Ptr* commences at the cellular blastoderm stage (Pastenes et al., 2008; Zúñiga et al., 2009) and reaches its highest level later during embryonic development (modENCODE, Brown et al., 2014). During gastrulation, the distribution of Ptr follows the typical pattern of pair-rule genes (Zúñiga et al., 2009) and in later stages is expressed in several tissues, including hemocytes (Bolatto et al., 2015; Cattenoz et al., 2020). Results from an *in vitro* assay suggested that Ptr could compete with Ptc for the ligand Hh, thereby serving as an additional modulator of Hh signaling (Bolatto et al., 2022). Loss of function in *Ptr* causes high embryonic mortality and nervous system alterations (Bolatto et al., 2022; Zhao et al., 2008) but the precise molecular function of Ptr remains elusive.

Our investigation sought to elucidate specific contributions of Ptr to *D. melanogaster* development, with a particular emphasis on its effects on post-embryonic survival, larval locomotion, and adult lifespan. To achieve this, we employed a null mutant model ($Ptr^{23c}$, Bolatto et al., 2015). We found that $Ptr^{23c}$ mutants reaching the end of embryonic development often die due to an inability to hatch. The few individuals that reach the larval stage are lethargic and exhibit abnormal muscle nuclei. Despite these challenges, a small proportion of $Ptr^{23c}$ mutants manage to develop to the adult stage and notably, they exhibit extended lifespan. Our findings shed light on the intricate interplay between Ptr function and the phenotypic outcomes observed throughout the life stages of *D. melanogaster*.

## Results

Our investigation began focusing on the effect of the null mutation $Ptr^{23c}$ on survival through multiple stages of pre-adult development. Ptr is essential for embryonic survival because mutants generated by P-element excision (Bolatto et al., 2015) exhibit a mortality rate of 81% during embryogenesis (Bolatto et al., 2022). We found that RNAi-induced knockdown under the control of a maternally expressed alphaTub67C promoter caused between 10% to 46% of mortality during embryonic development (data not shown). Later in embryogenesis, by stage 17, $Ptr^{23c}$ embryos exhibited a reduced hatching index compared to control embryos of the same age (median: control 96%, mutant 79%, $p < 0.05$) (Fig. 1A). Careful examination revealed that mutants lived for up to 24 additional hours and showed peristaltic contractions but failed to hatch and died within the egg shell.

When raised in standard culture medium, most *Ptr*$^{23c}$ larvae die before molting into the second instar. We found that it was possible to keep these mutants alive by culturing them on a soft apple juice-agar medium supplemented with yeast. In these conditions, although mutant larvae experienced a significant reduction in survival rate compared to controls, some individuals completed larval development and reached the pupal stage (median: control 83%, mutant 13%, $p < 0.01$) (Fig. 1B). A significant decrease in survival was also observed at the pupal stage when mutants were compared with control pupae (median: control 100%, mutant 33%, $p < 0.0001$), as determined by the Mann-Whitney test (Fig. 1C). Some mutant pupae reached the final stage of pre-adult development as fully formed pharate adults. Remarkably, a significant sex effect of the *Ptr*$^{23c}$ mutation was observed, with a much lower proportion of females reaching this stage (mean: control males 54.2% and females 45.8%; mutant males 87.3%, females 12.7%, $p < 0.01$) (Fig. 1D). The exceptionally low proportion of mutant females reaching the adult stage posed a challenge for assessing lifespan in individuals of this sex. Consequently, our analysis of adult lifespan was limited to males.

The small subset of *Ptr*$^{23c}$ mutants that survived into adulthood exhibited an extended lifespan compared with control flies (median = 50 days vs. 34 days). Kaplan-Meier analysis revealed significant differences ($p < 0.0001$) in both the Gehan-Breslow-Wilcoxon and Mantel-Cox tests (Fig. 1E).

We observed that *Ptr*$^{23c}$ larvae exhibited a lethargic behavior. When assayed with a locomotion test early in larval development (first instar) mutant larvae had a significantly reduced locomotion (19.8 mm) compared to control larvae (36.5 mm, Fig 2A). Additionally, mutant larvae moved at a 54% slower median speed (0.45 mm/sec) compared with control larvae (0.83 mm/sec Fig. 2B). Towards the end of larval life (third instar), mutant larvae continued to show deficient locomotion (154.5mm; 3.51 mm/sec) relative to control larvae (224.8; 5.11 mm/sec), although the differences were diminished to a 68% from that of the control.

Hatching and locomotion depend on the interaction between the nervous system and the musculature (Baker et al., 2018; Crisp et al., 2008; Hunter et al., 2021). While abnormal nervous system morphology has been reported for *Ptr* mutants (Zhao et al., 2008; Bolatto et al., 2022), the possibility of abnormal musculature has not yet been investigated. To address this issue, we utilized F-actin and DNA staining to examine the somatic muscles of *Ptr*$^{23c}$ mutant third-instar larvae. Our analysis revealed a mutant phenotype characterized by enlarged cell nuclei in all muscles (Fig. 2E-G, median area: control = 99.8 $\mu m^2$, *Ptr*$^{23c}$ = 127.1 $\mu m^2$).

## Discussion

Ptr plays a critical role during early development, evidenced by the fact that *Ptr*$^{23c}$ mutants exhibit a high mortality rate during embryogenesis (Bolatto et al., 2022). We developed a culture strategy which allowed some mutant individuals to complete larval and pupal development and reach the adult stage, providing the means to study the effect of the *Ptr* mutation during this life stage. Through comprehensive analysis of the post-embryonic mutant phenotype and the evaluation of putative enhancers of *Ptr*, we propose an interaction of Ptr with the insulin pathway.

We observed a reduction in larval hatching and impaired locomotion in mutant larvae. Both hatching of the larva from the eggshell and larval locomotion requires well-coordinated and strong muscle contractions controlled by the nervous system through sophisticated motor programs (Crisp et al., 2008; Baker et al., 2018; Hunter et al., 2021). Thereby, neuromuscular dysfunction provides a plausible explanation for the observed mortality caused by the *Ptr*$^{23c}$ mutation at embryonic and larval stages.

Although not addressed in this study, we consider that the incremented mortality of mutant pupae could be also associated with deficient neuromuscular function because ecdysis involves abdominal muscular contractions driving head eversion and expansion of wing pads and legs (Kim et al., 2006). By the end of the pupal period, after larval muscles undergo massive histolysis, adult muscles differentiate (Preethi and Krzysztof, 2020; Kuleesha et al., 2016). Muscle activity occurs during fly eclosion from the pupal case (adult ecdysis Elliott et al., 2021). Interestingly, we found mortality in both early and late pupal stages (data not shown), with the highest mortality being detected in *Ptr*$^{23c}$ female pupae. Although we did not explore causation, notably, the sex differences in adult mortality observed here correlate with sex differences in *Ptr* expression. A higher expression of *Ptr* in the central nervous system of females was reported using RNAseq analysis (Leader et al., 2018, *flyatlas2.org*). Sexual dimorphism in *Drosophila* is regulated by different genes. The female sex determinant, *Sex-lethal*, is expressed in two distinct neuronal subpopulations within the central nervous system, one of which corresponds to insulin-producing cells. This sex difference in the production of insulin-like peptides could act globally in tissue growth (Sawala and Gould, 2017). It is also known that insulin-like peptides regulate pupal nervous system development and ecdysis

(Truman and Riddiford, 2023).

The contrast between high pre-adult mortality and extended adult lifespan among the few escapers prompts further exploration of the complex interplay of factors influencing the life history of *Ptr*$^{23c}$ mutants. Genome-wide analysis of single-nucleotide polymorphisms demonstrated that *Ptr* resides in one of the genomic regions associated with longevity (Durham et al., 2014). Nutrient signaling pathways are implicated on extended *Drosophila* lifespan, where signals secreted from the gut, fat and muscle tissues trigger protective effects across the whole organism (reviewed in Piper and Partridge, 2018). Our unexpected observation of extended adult life within *Ptr* mutant males raises intriguing questions about the underlying mechanisms and potential connections with the metabolic processes commented below.

Noteworthy, the muscular phenotype observed here in *Ptr*$^{23c}$ mutants suggests the possibility of a link between Ptr-mediated Hh signaling and muscle development. During larval growth, nuclear endoreplication of somatic muscles is under intricate control mechanisms including the interplay of Hh antagonistic signaling from the insulin receptor (InR) and dFOXO pathways (Demontis & Perrimon 2009; Singh et al., 2018). Data from ovary follicle stem cells evidence antagonistic effects between the insulin and Hh signaling pathways, with Hh dependent autophagy being inhibited by insulin activation (Singh et al., 2018).

Some hints arise from gut epithelial cells, where it is well established that endocycle regulation relies on both Tor-dependent InR signaling and Tor-independent EGFR/MAPK signaling (Xiang et al., 2017). Additionally, Hh is released from gut enterocytes under starvation conditions (Rodenfels et al., 2014), where several genes controlling endoreplication are activated by the Hh signaling pathway (Fuß et al., 2001). Using an experimental paradigm involving larvae reared in a nutrient-restricted medium (Singh et al., 2018) to inhibit InR signaling we found a potential involvement of Tor-independent mechanisms in promoting the muscular endocycle. Therefore, the muscular phenotype observed here in *Ptr*$^{23c}$ larvae suggests that the loss of function in *Ptr* could perhaps enhance a MAPK-dependent pathway or release some inhibition. Furthermore, mild muscle mitochondrial distress may be associated with increased lifespan via the potential repression of systemic insulin signaling as suggested by previous studies (Owusu-Ansah et al., 2013).

Further clues emerge from the identification of putative enhancers of *Ptr* through the TF2DNA database (Pujato et al., 2014), indicating the transcription factors Escargot (Esg) and Ken as potential regulators. Esg, a master regulator of intestinal stem cells (Khanbabei et al., 2024), exerts an inhibitory role in the InR pathway (Sênos Demarco et al., 2022), controls

ploidy (Fuse et al., 1994), and is regulated by the Jak/STAT pathway (Chatterjee et al., 2023). Meanwhile, Ken acts as a negative regulator of the Jak/STAT pathway (Arbouzova et al., 2006), and controls self-renewal in the testis by repressing differentiation (Issigonis and Matunis, 2012). Hence, we propose that the transcription factors Esg and Ken might provide a molecular link between Ptr and Jak/STAT signaling.

Potential interactions between the InR/Foxo pathway, Hh signaling, and insulin-IGF pathways, in line with existing literature (Hwangbo et al., 2004; Singh et al., 2018) might underlie the phenotype we observed in the $Ptr^{23c}$ mutant. However, the intricacies of these interactions require further exploration.

**Conclusions**

Our study provides critical insights into the multifaceted role of *Ptr* throughout the entire life cycle of *Drosophila melanogaster*. The high mortality during embryonic, larval and pupal stages, the deficient locomotion of the larvae and the unexpected extension of adult lifespan in *Ptr* null mutants offer a complex picture that confirms the importance of Ptr for normal development and requires further exploration. Our findings also open avenues for investigating the broader genetic networks governing these intricate processes.

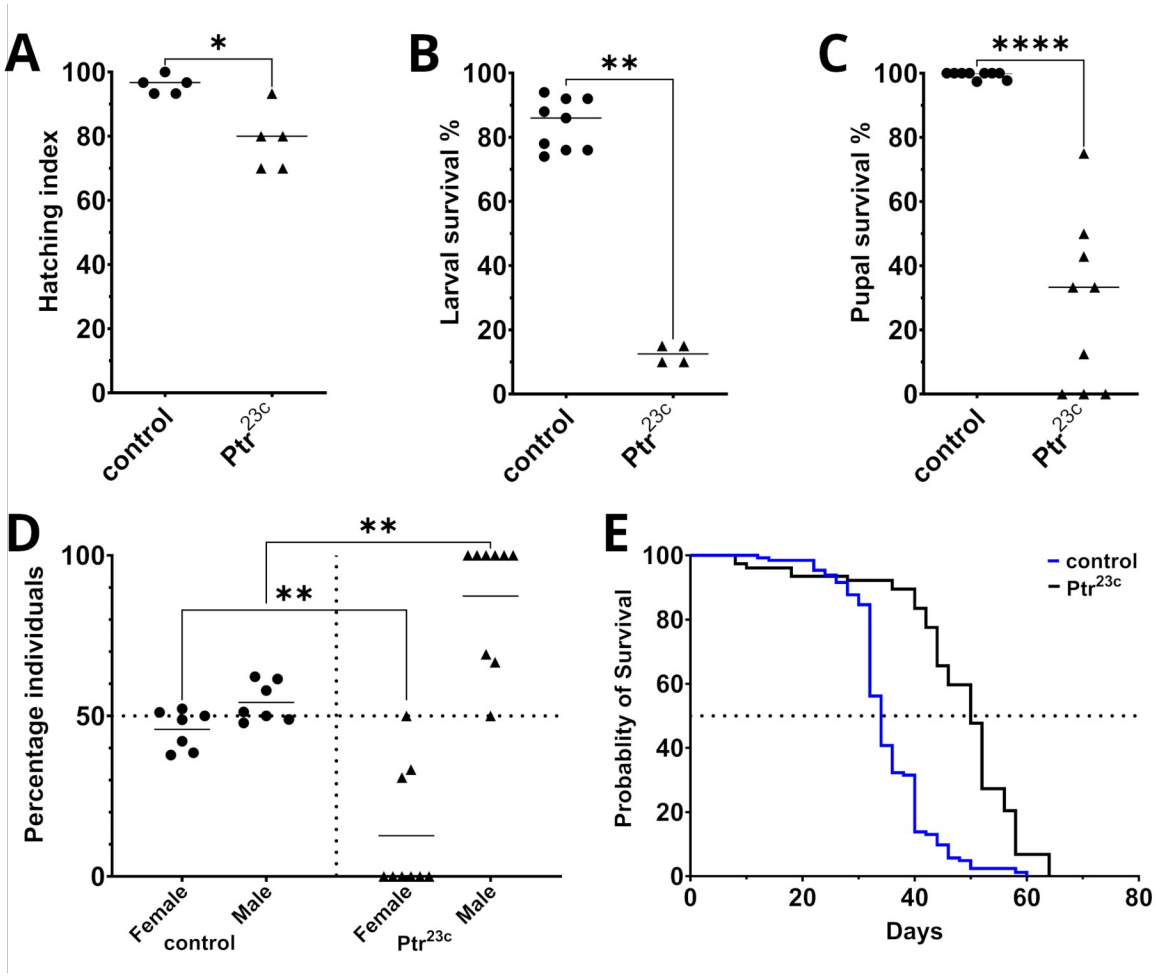


**Figure 1. The Ptr$^{23c}$ mutation affects survival at every stage of the life cycle of *Drosophila*. (A)** Reduced larval hatching among Ptr$^{23c}$ mutants. Hatching index was calculated, Median: control 96%, mutant 79%; n = 5 plates with 30 embryos each; $p < 0.05$. **(B)** Reduced survival of larvae among Ptr$^{23c}$ mutants. A very low proportion of mutant larvae reach the pupal stage. Median: control 83%, mutant 13%; n = minimum of 4 plates with 40 larvae each; $p < 0.01$. **(C)** Reduced mutant survival along the pupal stage. Median: control 100%, mutant 33%; $p < 0.0001$, assessed by Mann-Whitney test. n = 9 cages with pupae each. **(D)** Proportion of individuals of each sex at the pupal stage, showing a significant sex disparity in the mutant. Mean: control males 54%, females 46%; mutant males 87%, females 13%; n = 7 (control) and 9 (mutant) cages each. $p < 0.01$. **(E)** *Ptr$^{23c}$* mutant adult males exhibited extended lifespan (median: 50 days) compared to control males (median: 34 days). Significant differences revealed by Kaplan-Meier analysis ($p < 0.0001$) in Gehan-Breslow-Wilcoxon and Mantel-Cox tests; Chi-squared = 59.6. N = 100 flies (control) and 22 flies (mutants).

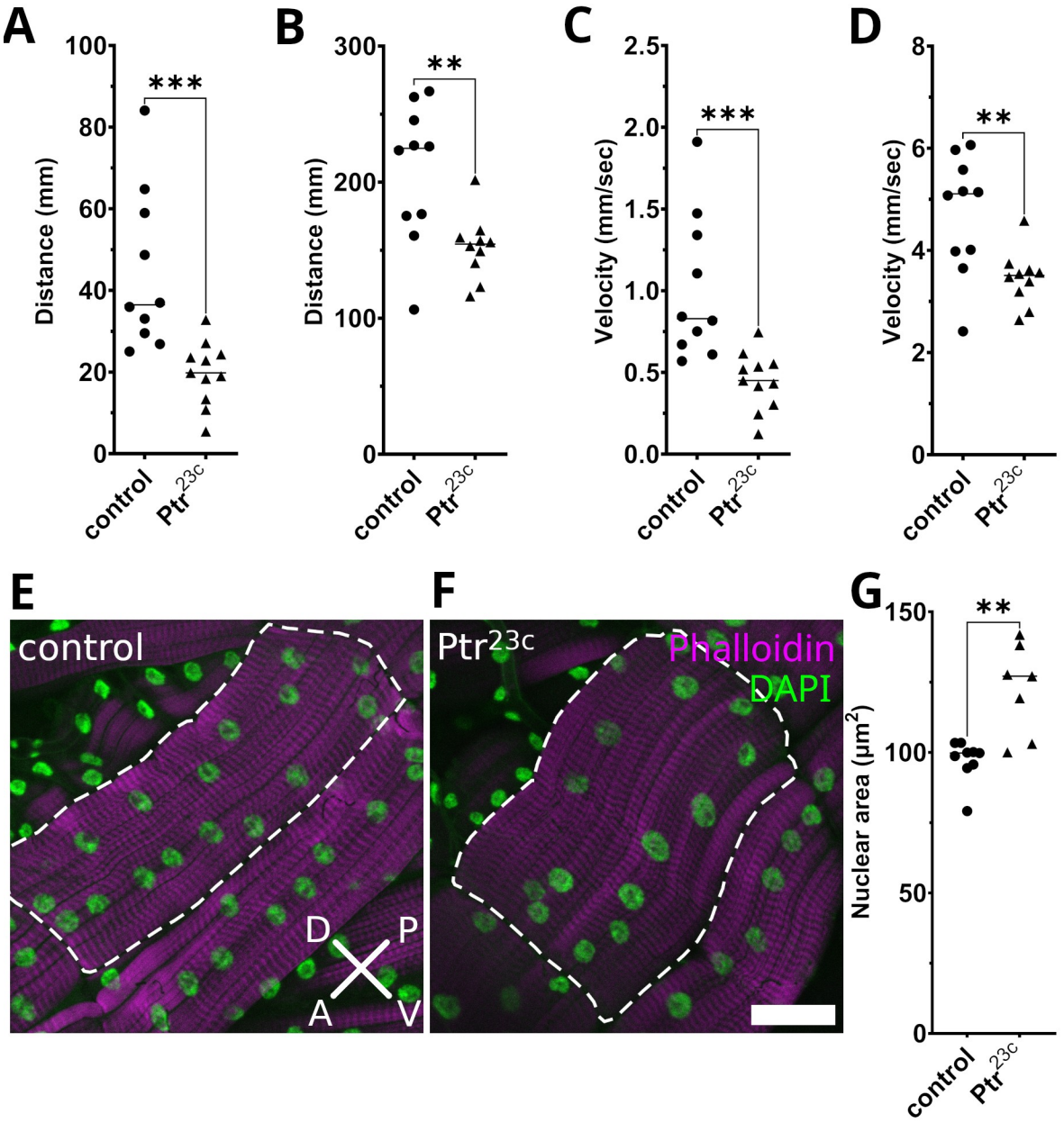


**Fig. 2: Locomotion and muscular phenotype associated with *Ptr* loss of function.** Motor impairment in *Ptr*$^{23c}$ mutant larvae **(A-D)** correlates with a muscular phenotype **(E-G)**. **(A)** The *Ptr*$^{23c}$ mutation reduced the crawling distance covered by first-instar larvae during 45 sec from 27.4 mm in control larvae (n=10) to 19.8 mm in *Ptr*$^{23c}$ (n=11). **(B)** Third-instar mutant larvae showed reduced crawling distance from 224 mm, 160.5 mm, n=10 (control larvae) to 154 mm, 85.6 mm, n=10. Crawling velocity was also reduced **(C)** from 0.83 mm/sec (control larvae) to 0.45 mm/sec for first instar larvae and **(D)** from 5.11 mm/sec (control larvae) to 3.51 mm/sec for third-instar larvae (Medians are shown in A to D). Statistical significance was determined using the Mann-Whitney U-test, yielding a p-value < 0.001 and 0.01. **(E-F)** Confocal laser scanning microscopy images of somatic muscle VL3 (dashed line) showing nuclei in green and F-actin in magenta. Maximum intensity projection images from a

representative control larva **(E)** and a *Ptr*$^{23c}$ mutant larva (**F**). Scale bar: 50 µm (20 planes at 0.5 µm intervals along the z axis). **(G)** Nuclear size evaluation through the measurement of nuclear area on maximum intensity z-projections of confocal stacks from body wall preparations. Statistical analysis, performed using the Mann-Whitney U-test, revealed that the area of muscle nuclei was 27% larger in the mutant compared to control. Median: control 99.8 $\mu m^2$, mutant 127.1 $\mu m^2$; p-value < 0.01. VL3 abdominal muscle was used for quantification. n= 9 control and 7 mutant larvae. IQR: Interquartile range; A: anterior; P: posterior; V: ventral; D: dorsal.

## Materials and Methods

### Genetics and *Drosophila* strains

*Drosophila melanogaster* strains were obtained from the following sources: *w;Df(2L)32FP-5/CyO,twist-Gal4,UAS-GFP* (Pirone 2016); *w*; He-GAL4.Z, UAS-GFP.nls* (#8700, BDSC); *w*, Bl/CyO; TM2/TM6b* balancer, *Ptr*$^{23c}$*/CyO, ftz-lacZ* (Bolatto et al., 2015). Crosses were performed following standard procedures. Flies were maintained on standard cornmeal/yeast/glucose medium at 25°C, with 12h/12h dark/light cycles. These stocks were used to generate the *Ptr*$^{23c}$*/CyO, twi-GFP* and the *Ptr*$^{23c}$*/CyO, twi-GFP; He-GFP/He-GFP* strains, of which the latter was used for lifespan experiments. As control we used the wild-type strain Oregon-R and +/+; *He-GFP/He-GFP* when appropriate. Control and mutant larvae selected for experiments were cultured in apple juice-agar medium supplemented with yeast.

### Embryo collection

Flies of the designated genotype were allowed to lay eggs on apple juice-agar plates supplemented with yeast. After an appropriate oviposition period, eggs were delicately collected using a brush and subsequently washed with tap water. De-chorionation was achieved by immersing the eggs in a 50% sodium hypochlorite solution followed by rinsing with PBST (0.05% Triton X100 in phosphate-buffered saline). Embryonic stages were determined according to morphological criteria (Campos-Ortega and Hartstein, 1997). When necessary, embryos were selected based on GFP fluorescence (see below).

### Hatching index

Groups of 30 late stage 17 embryos were transferred to apple juice-agar plates. The number of hatched and not hatched larvae was counted after 24 hours and the hatching index was

determined as Hatching index = Hatched larvae/Total larvae.

**Measurement of larval locomotion**

To analyze neuromuscular function, larvae were recorded during 45 sec on video under the dissecting microscope. Two aspects of larval locomotion were assessed, crawled distance and crawling velocity, using the Manual Tracking plugin from FIJI, following methods outlined in Balakrishnan et al., 2021.

**Measurement of lifespan**

For lifespan measurements, 100 males of the control strain were kept in 10 vials, and 22 $Ptr^{23c}$ mutant males were kept in 4 vials. The dead flies were counted every 2 days and thereafter the living flies were transferred to fresh food every 2–4 days. Flies were maintained on cornmeal medium at 25 °C with 12:12 h light:darkness cycles as previously described (Ferreiro et al., 2018).

**Staining of larval somatic muscles**

To analyze the morphology of somatic muscles, third-instar larvae were dissected along the dorsal midline in ice-cold PBS. The viscera were removed and the resulting body-wall preparations were stretched and incubated in 0.5 mM EGTA for 5 min to obtain relaxed muscles at the start of fixation. Body walls were fixed in 4% paraformaldehyde (PFA) at room temperature for 15 minutes. After a double wash in PBS-T (0.3% Triton X-100 in PBS), body-wall preparations were incubated overnight with DAPI (1 µg/ml) and eosin-conjugated Phalloidin (1:200, Molecular Probes) at 4°C to visualize cell nuclei and F-actin, respectively. Subsequently, the body-wall preparations were mounted in 80% glycerol buffered with 1 mM Tris-HCl at pH=8. Images were taken of VL3 muscles of the 5$^{th}$ abdominal segment for nuclear area quantification.

**Microscopy and Imaging**

Fluorescent embryos were selected using a Wesco m300 series stereo microscope (USA) equipped with a Nightsea SFA fluorescence adapter (Nightsea, Hatfield, PA, USA). Locomotion assays were imaged using a mobile phone camera with a 3D-printed ocular adapter (https://www.instructables.com/Universal-Phone-MountAdapter-for-Microscope-Telesc/). Muscle images were acquired with a Zeiss LSM800 laser-scanning confocal

microscope using an EC Plan-Neofluar 20x/0.50 M27 objective and a 1.3X zoom using a GaAsP-PMT detector. Pinhole apertures were set at 29 µm for DAPI and 38 µm for Eosin-conjugated Phalloidin. Z-stacks of 1024x1024px images were taken at 500 nm steps. Subsequent image processing was performed using FIJI where the nuclear area was quantified on maximum intensity projections of z-stacks. Figures were crafted using Inkscape 1.1 (Inkscape Project, 2020) and GIMP 2.10 (The GIMP Development Team, 2019).

**Evaluation of putative enhancers of Ptr,**

For the identification of putative regulatory sequences we utilized the enhancers database (TF2DNA database, Pujato et al., 2014) available at https://www.fiserlab.org/tf2dna_db/. We conducted a search using the term 'Ptr', included a search for conserved domains in the query gene sequence and studied the resulting list of putative enhancers.

**Quantification and Statistical Analysis**

Data analyses were conducted using GraphPad Prism version 9.5. Statistical comparisons were performed employing Mann-Whitney U-test with a significance level set at $p<0.05$. Survival probabilities were calculated using Gehan-Breslow-Wilcoxon and Mantel-Cox tests.

**Author Contributions**

CP and DP designed the study. CP performed the experiments and prepared the figures. CP, DP and RC wrote the manuscript and analyzed the data. All authors contributed to the article and approved the submitted version.

**Funding**

This work was partially funded by a CSIC grant conferred to CP (CSIC Iniciación a la Investigación, 2017, ID216), funds from PEDECIBA (Programa de Desarrollo de las Ciencias Básicas) and funds granted to the Departamento de Biología del Neurodesarrollo (IIBCE, Montevideo).

**Acknowledgements**

The authors would like to thank Dr. María José Ferreiro for fruitful discussions and expert advice; Dr. Rosa Barrio for kindly providing the *w;Df(2L)32FP-5/CyO,twist-Gal4,UAS-GFP* stock, and Dr. Carmen Bolatto for kindly providing the $Ptr^{23c}$*/CyO, ftz-lacZ* stock.

## References


Arbouzova, N.I., Bach, E.A., Zeidler, M.P., 2006. Ken & Barbie selectively regulates the expression of a subset of JAK/STAT pathway target genes. Curr. Biol. 16, 80–88. https://doi.org/10.1016/j.cub.2005.11.033

Baker, R., Nakamura, N., Chandel, I., Howell, B., Lyalin, D., Panin, V.M., 2018. Protein O-Mannosyltransferases affect sensory axon wiring and dynamic chirality of body posture in the *Drosophila* embryo. J. Neurosci. 38, 1850–1865. https://doi.org/10.1523/JNEUROSCI.0346-17.2017

Bolatto, C., Nieves, S., Reyes, A., Olivera-Bravo, S., Cambiazo, V., 2022. Patched-Related Is required for proper development of embryonic *Drosophila* nervous system. Front. Neurosci. 16, 920670. https://doi.org/10.3389/fnins.2022.920670

Bolatto, C., Parada, C., Revello, F., Zuñiga, A., Cabrera, P., Cambiazo, V., 2015. Spatial and temporal distribution of Patched-related protein in the *Drosophila* embryo. Gene Expr. Patterns 19, 120–128. https://doi.org/10.1016/j.gep.2015.10.002

Brown, J.B., Boley, N., Eisman, R., May, G.E., Stoiber, M.H., Duff, M.O., Booth, B.W., Wen, J., Park, S., Suzuki, A.M., Wan, K.H., Yu, C., Zhang, D., Carlson, J.W., Cherbas, L., Eads, B.D., Miller, D., Mockaitis, K., Roberts, J., Davis, C.A., Frise, E., Hammonds, A.S., Olson, S., Shenker, S., Sturgill, D., Samsonova, A.A., Weiszmann, R., Robinson, G., Hernandez, J., Andrews, J., Bickel, P.J., Carninci, P., Cherbas, P., Gingeras, T.R., Hoskins, R.A., Kaufman, T.C., Lai, E.C., Oliver, B., Perrimon, N., Graveley, B.R., Celniker, S.E., 2014. Diversity and dynamics of the *Drosophila* transcriptome. Nature 512, 393–399. https://doi.org/10.1038/nature12962

Cattenoz, P.B., Sakr, R., Pavlidaki, A., Delaporte, C., Riba, A., Molina, N., Hariharan, N., Mukherjee, T., Giangrande, A., 2020. Temporal specificity and heterogeneity of *Drosophila* immune cells. EMBO J. 39. https://doi.org/10.15252/embj.2020104486

Chatterjee, D., Cong, F., Wang, X.-F., Machado Costa, C.A., Huang, Y.-C., Deng, W.-M., 2023. Cell polarity opposes Jak/STAT-mediated Escargot activation that drives intratumor heterogeneity in a *Drosophila* tumor model. Cell Rep. 42, 112061. https://doi.org/10.1016/j.celrep.2023.112061

Crisp, S., Evers, J.F., Fiala, A., Bate, M., 2008. The development of motor coordination in *Drosophila* embryos. Development 135, 3707–3717. https://doi.org/10.1242/dev.026773

Demontis, F., Perrimon, N., 2009. Integration of Insulin receptor/Foxo signaling and dMyc activity during muscle growth regulates body size in *Drosophila*. Development 136, 983–993. https://doi.org/10.1242/dev.027466

Durham, M.F., Magwire, M.M., Stone, E.A., Leips, J., 2014. Genome-wide analysis in *Drosophila* reveals age-specific effects of SNPs on fitness traits. Nat. Commun. 5, 4338. https://doi.org/10.1038/ncomms5338

Elliott, A.D., Berndt, A., Houpert, M., Roy, S., Scott, R.L., Chow, C.C., Shroff, H., White, B.H., 2021. Pupal behavior emerges from unstructured muscle activity in response to neuromodulation in *Drosophila*. eLife 10, e68656. https://doi.org/10.7554/eLife.68656

Ferreiro, M. J., Pérez, C., Marchesano, M., Ruiz, S., Caputi, A., Aguilera, P., Barrio, R., Cantera, R., 2018. *Drosophila melanogaster* white mutant $w^{1118}$ undergo retinal degeneration. Frontiers in neuroscience, 11, 732. https://doi.org/10.3389/fnins.2017.00732

Fuse, N., Hirose, S., Hayashi, S., 1994. Diploidy of *Drosophila* imaginal cells is maintained by a transcriptional repressor encoded by *escargot*. Genes Dev. 8, 2270–2281. https://doi.org/10.1101/gad.8.19.2270

Fuß, B., Meißner, T., Bauer, R., Lehmann, C., Eckardt, F., Hoch, M., 2001. Control of endoreduplication domains in the *Drosophila* gut by the knirps and knirps-related genes. Mech. Dev. 100, 15–23. https://doi.org/10.1016/S0925-4773(00)00512-8

Hunter, I., Coulson, B., Zarin, A.A., Baines, R.A., 2021. The *Drosophila* larval locomotor circuit provides a model to understand neural circuit development and function. Front. Neural Circuits 15, 684969. https://doi.org/10.3389/fncir.2021.684969

Hwangbo, D.S., Gersham, B., Tu, M.-P., Palmer, M., Tatar, M., 2004. *Drosophila* dFOXO controls lifespan and regulates insulin signalling in brain and fat body 429. https://doi.org/10.1038/nature02549

Issigonis, M., Matunis, E., 2012. The *Drosophila* BCL6 homolog ken and barbie promotes somatic stem cell self-renewal in the testis niche. Dev. Biol. 368, 181–192. https://doi.org/10.1016/j.ydbio.2012.04.034

Khanbabei, A., Segura, L., Petrossian, C., Lemus, A., Cano, I., Frazier, C., Halajyan, A., Ca, D., Loza-Coll, M., 2024. Experimental validation and characterization of putative targets of Escargot and STAT, two master regulators of the intestinal stem cells in *Drosophila melanogaster*. Dev. Biol. 505, 148–163. https://doi.org/10.1016/j.ydbio.2023.10.008

Kim, Y. J., Zitnan, D., Galizia, C. G., Cho, K. H., Adams, M. E., 2006. A command chemical triggers an innate behavior by sequential activation of multiple peptidergic ensembles. Current biology : CB, 16(14), 1395–1407. https://doi.org/10.1016/j.cub.2006.06.027

Kuleesha, Y., Puah, W.C., Wasser, M., 2016. Live imaging of muscle histolysis in *Drosophila*

metamorphosis. BMC Dev. Biol. 16, 12. https://doi.org/10.1186/s12861-016-0113-1

Leader, D.P., Krause, S.A., Pandit, A., Davies, S.A., Dow, J.A.T., 2018. FlyAtlas 2: a new version of the *Drosophila melanogaster* expression atlas with RNA-Seq, miRNA-Seq and sex-specific data. Nucleic Acids Res. 46, D809–D815. https://doi.org/10.1093/nar/gkx976

Owusu-Ansah, E., Song, W., Perrimon, N., 2013. Muscle mitohormesis promotes longevity via systemic repression of insulin signaling. Cell 155, 699–712. https://doi.org/10.1016/j.cell.2013.09.021

Pastenes, L., Ibáñez, F., Bolatto, C., Pavéz, L., Cambiazo, V., 2008. Molecular characterization of a novel patched-related protein in *Apis mellifera* and *Drosophila melanogaster*. Arch. Insect Biochem. Physiol. 68, 156–170. https://doi.org/10.1002/arch.20245

Piper, M.D.W., Partridge, L., 2018. *Drosophila* as a model for ageing. Biochim. Biophys. Acta BBA - Mol. Basis Dis. 1864, 2707–2717. https://doi.org/10.1016/j.bbadis.2017.09.016

Poovathumkadavil, P., Jagla, K., 2020. Genetic Control of Muscle Diversification and Homeostasis: Insights from *Drosophila*. Cells, 9(6), 1543. https://doi.org/10.3390/cells9061543

Pujato, M., Kieken, F., Skiles, A.A., Tapinos, N., Fiser, A., 2014. Prediction of DNA binding motifs from 3D models of transcription factors; identifying TLX3 regulated genes. Nucleic Acids Res. 42, 13500–13512. https://doi.org/10.1093/nar/gku1228

Rodenfels, J., Lavrynenko, O., Ayciriex, S., Sampaio, J.L., Carvalho, M., Shevchenko, A., Eaton, S., 2014. Production of systemically circulating Hedgehog by the intestine couples nutrition to growth and development. Genes Dev. 28, 2636–2651. https://doi.org/10.1101/gad.249763.114

Sawala, A., Gould, A. P., 2017. The sex of specific neurons controls female body growth in *Drosophila*. PLoS biology, *15*(10), e2002252. https://doi.org/10.1371/journal.pbio.2002252

Sênos Demarco, R., Stack, B.J., Tang, A.M., Voog, J., Sandall, S.L., Southall, T.D., Brand, A.H., Jones, D.L., 2022. Escargot controls somatic stem cell maintenance through the attenuation of the insulin receptor pathway in *Drosophila*. Cell Rep. 39, 110679. https://doi.org/10.1016/j.celrep.2022.110679

Singh, T., Lee, E.H., Hartman, T.R., Ruiz-Whalen, D.M., O'Reilly, A.M., 2018. Opposing action of hedgehog and insulin signaling balances proliferation and autophagy to determine follicle stem cell lifespan. Dev. Cell 46, 720-734.e6.

https://doi.org/10.1016/j.devcel.2018.08.008

Truman, J. W., Riddiford, L. M., 2023. *Drosophila* postembryonic nervous system development: a model for the endocrine control of development. Genetics, 223(3), iyac184. https://doi.org/10.1093/genetics/iyac184

Xiang, J., Bandura, J., Zhang, P., Jin, Y., Reuter, H., Edgar, B.A., 2017. EGFR-dependent TOR-independent endocycles support *Drosophila* gut epithelial regeneration. Nat. Commun. 8, 15125. https://doi.org/10.1038/ncomms15125

Zhao, T., Gu, T., Rice, H.C., McAdams, K.L., Roark, K.M., Lawson, K., Gauthier, S.A., Reagan, K.L., Hewes, R.S., 2008. A *Drosophila* Gain-of-Function Screen for Candidate Genes Involved in Steroid-Dependent Neuroendocrine Cell Remodeling. Genetics 178, 883–901. https://doi.org/10.1534/genetics.107.082487

Zúñiga, A., Hödar, C., Hanna, P., Ibáñez, F., Moreno, P., Pulgar, R., Pastenes, L., González, M., Cambiazo, V., 2009. Genes encoding novel secreted and transmembrane proteins are temporally and spatially regulated during *Drosophila melanogaster* embryogenesis. BMC Biol. 7, 61. https://doi.org/10.1186/1741-7007-7-61